P-ISSN 2586-9000
E-ISSN 2586-9027
Homepage : https://tci-thaijo.org/index.php/SciTechAsia
Science & Technology Asia
Vol. 28 No.3 July – September 2023
Page: [1-17]
Original research article

Williamson Fluid Flow Having Microorganisms Over a Permeable Shrinking Sheet

Nepal Chandra Roy[1], Goutam Saha[1,*], Suvash C. Saha[2]

[1]*Department of Mathematics, University of Dhaka, Dhaka 1000, Bangladesh*
[2]*School of Mechanical & Mechatronic Engineering, University of Technology Sydney, NSW 2007, Australia*

Received 6 January 2023; Received in revised form 25 April 2023
Accepted 6 June 2023; Available online 26 September 2023

ABSTRACT

This study examines the characteristics of fluid flow of microorganisms over a permeable vertical shrinking sheet in the presence of a magnetic field and thermal radiation. The governing equations are simplified to a nonlinear system of ODEs and solved using the nonlinear shooting method. The results of the study show that an increase in certain parameters, such as the Eckert number and Hartmann number, leads to an increase in local skin friction coefficient and density of microorganisms, and a decrease in the local Nusselt number. However, when the Weissenberg number is higher, the opposite characteristics are observed. The study also found that the domain of dual solutions increases with the increase of certain parameters but decreases with a higher Weissenberg number and boundary layer separation is delayed with the increase of dual solutions.

Keywords: Boundary layer; Dual solutions; Microorganisms; Shrinking sheet; Williamson fluid

1. Introduction

Williamson fluid is well known as non-Newtonian fluid and it has been a research interest of many researchers for several decades. It has many applications in industrial and engineering areas, such as bio-fluids, biomedical engineering, nuclear plants, reducing frictions, etc. Also, the effect of microorganisms is another research area that has gained extensive interest recently by researchers. The reason behind this fact is that microorganisms such as bacteria, protozoa, and viruses are available almost everywhere in nature and we have overlooked their presence in the fluids. So, it is really important to see the significance of the presence of micro-organisms on the fluid's flow and heat transfer. In the following, we will focus on articles that showed attention to Williamson fluid and also used microorganisms in their research.

***Corresponding author:** gsahamath@du.ac.bd

Nadeem and Hussain [1] studied analytically to understand the fluid flow and heat transfer features of nano Williamson fluid over a stretching surface using the Homotopy analysis method. They considered some important parameters such as Williamson parameters (*We*), Lewis number (*Le*), and Schmidt number (*Sc*). They observed that these parameters can influence the augmentation of heat transfer. Krishnamurthy et al. [2] presented numerically the flow of Williamson fluid over the horizontal stretching impermeable sheet with the presence of a magnetic field. They used the nonlinear shooting method with Runge-Kutta-Fehlberg's (RKF) 4-5th technique to resolve the converted nonlinear non-dimensional system. They also considered some important parameters such as Prandtl (*Pr*), Stefan, and Lewis numbers (*Le*), radiation, Brownian motion, thermophoresis, chemical reaction, melting, permeability, magnetic, and Williamson parameters (*We*). They observed that Brownian motion and thermophoresis effects play an important role to increase Nu_x. Reddy et al. [3] investigated numerically the MHD Williamson nanofluid flow past a stretching sheet with the consideration of variable viscosity and thermal conductivity. They used the spectral quasi-linearisation method (SQLM) to resolve the transformed ODE's under some physical parameters such as Prandtl, Lewis, and Schmidt numbers, magnetic, radiation, and Williamson parameters. They found that variable thermal conductivity plays an important role to decrease the heat transfer coefficient. A similar study has been conducted by Ibrahim and Gamachu [4] and used the same method as mentioned by Reddy et al. [3]. Shawky et al. [5] investigated numerically the Williamson nanofluid flow past a stretching porous sheet with the consideration of some important effects such as Dufour, Soret, Brownian motion, and thermophoresis. They used the nonlinear shooting method with Runge-Kutta (RK) technique. They found that all the above-mentioned effects have a role in the increment of Nusselt number, but the Sherwood number plays the opposite role. Kho et al. [6] analyzed numerically the heat and mass transfer behavior of Williamson nanofluid flow past a stretching sheet. They used the method mentioned by Shawky et al. [5]. They observed that the Nu_x decreases with the increase of *Le* and *Pr*. Some relevant researches are also available in Zaib et al. [7, 8]. Most recently, Dawar et al. [9] investigated analytically the Williamson flow past a stretching plate using the Homotopy analysis method and presented their findings through graphs such as velocity and temperature. In their study, some important physical parameters such as *Pr*, *Sc*, and *Le* are considered. They observed that heat transfer is an increasing function of Pr and mass transfer rate decreased with the augmentation of *Le*. Mishra and Mathur [10] used a semi-analytical approach to examine the mass transfer analysis of Williamson nanofluid flow past a stretching porous sheet. They used the variation parameter method and investigated the characteristic of some effects such as Brownian motion, and thermophoresis. Their finding reveals that the above mentioned effects delay the progress of mass transfer rate. Ahmed and Akbar [11] numerically investigated the magnetohydrodynamics flow of Williamson nanofluid past an exponentially stretching permeable sheets with two different types of heat transfer cases. They used Matlab-based built-in solver bvp4c to solve the transformed system concerning some important parameters such as Prandtl and Schmidt numbers, magnetic, suction or injection, thermophoresis, Brownian motion, and Williamson parameters. They found that the wall temperature gradient has a negative influence with the increase of all the parameters except the Prandtl number. Qureshi [12] numerically studied the heat transfer and entropy behavior of MHD Williamson nanofluid flow past a flat stretching sheet using finite difference method (FDM). The author found that Cu-water nanofluid showed behavior than TiO2 nanofluid. Mehran et al. [13] carried out a numerical investigation of

nanofluid flow past a vertical plate with the consideration of microorganisms. They introduced the iterative FDM to discretize and solve the converted ODE. Their results show that enhancement of bio-convection Rayleigh number (Ra_b) and degeneration of bio-convection Lewis number (Le_b) reduce the rate of heat transfer. Biswas et al. [14] studied MHD flow in a lid-driven cavity with the presence of oxytactic microorganisms using the finite volume method (FDM). They observed that the increase of magnetic field parameters has a strong influence on flow and thermal fields as well as the distribution of microorganisms. Yusuf et al. [15] numerically investigated the entropy production of MHD Williamson nanofluid flow consisting of microorganisms past an inclined plate. They used a well-known shooting method to solve the converted nonlinear ODE. The major finding from this research is microorganisms' density decreased with the increase of bioconvection Peclet and Schmidt numbers. In addition, some recent studies related to dual solutions are discussed in [16, 17].

From the above literature review, it is seen that there exists no research on the dual solution of magnetohydrodynamics flow of Williamson fluid past a vertical permeable sheet with the existence of microorganisms. Hence, the goal of our research is to observe the dual solution behaviors of Williamson fluid flow over porous surface with microorganisms and Boussinesq approximation and also investigate the influence of some main parameters such as Hartman, Eckert, Dufour, Weissenberg, Brownian diffusivity number, radiation parameter, and suction parameter. It is very important to understand the dual solution behavior of $Re_x^{1/2}C_f$, $Re_x^{-1/2}Nu_x$, $Re_x^{-1/2}Sh_x$ and $Re_x^{-1/2}Nn_x$. So, we aim to focus on these behaviors and present our findings graphically and also in tabular form.

2. Mathematical Modelling

Consider 2D steady MHD Williamson fluid flows with the presence of microorganisms over a permeable surface as shown in Fig. 1.

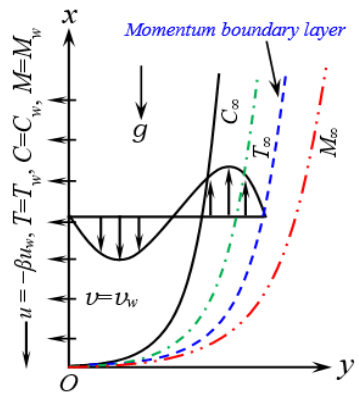

Fig. 1. Physical diagram of the geometry.

We assume that microorganisms are very small in size so that porosity holes will not create any impact on them. Assuming Boussinesq approximation, the flow, heat, mass transfer, and microorganisms of MHD Williamson fluid are presented by the following PDEs:

$$\frac{\partial u}{\partial x}+\frac{\partial v}{\partial y}=0, \tag{2.1}$$

$$\begin{aligned} &u\frac{\partial u}{\partial x}+v\frac{\partial u}{\partial y}=\nu\frac{\partial^2 u}{\partial y^2}\\ &+\sqrt{2}\nu\Gamma\frac{\partial u}{\partial y}\frac{\partial^2 u}{\partial y^2}-\left(\frac{\sigma B_0^2}{\rho}+\frac{\nu}{\kappa'}\right)\\ &+g\beta_T\left(T-T_\infty\right)+g\beta_C\left(C-C_\infty\right)\\ &+g\beta_M\left(M-M_\infty\right), \end{aligned} \tag{2.2}$$

$$\begin{aligned} &u\frac{\partial T}{\partial x}+v\frac{\partial T}{\partial y}=\frac{\nu}{C_p}\Phi+\frac{\kappa}{\rho C_p}\frac{\partial^2 T}{\partial y^2}\\ &+\frac{D_m\bar{\kappa}}{C_s C_p}\frac{\partial^2 C}{\partial y^2}+\tau D_B\frac{\partial T}{\partial y}\frac{\partial C}{\partial y}\\ &+\frac{\tau D_T}{T_\infty}\left(\frac{\partial T}{\partial y}\right)^2-\frac{1}{\rho C_p}\frac{\partial q_r}{\partial y}, \end{aligned} \tag{2.3}$$

$$u\frac{\partial C}{\partial x}+v\frac{\partial C}{\partial y}=D_B\frac{\partial^2 C}{\partial y^2}+\frac{D_T}{T_\infty}\frac{\partial^2 T}{\partial y^2}, \tag{2.4}$$

$$u\frac{\partial M}{\partial x}+v\frac{\partial M}{\partial y}+\frac{bv_C}{C_\infty}\frac{\partial}{\partial y}\left(M\frac{\partial C}{\partial y}\right)=D_n\frac{\partial^2 M}{\partial y^2}, \tag{2.5}$$

subject to the following boundary conditions:

$$u = -\beta u_w(x) = -\beta b\left(\frac{x}{l}\right), \quad v = v_w \text{ at } y = 0, \tag{2.6}$$

$$u \to 0 \text{ as } y \to \infty, \tag{2.7}$$

$$T = T_w = T_\infty + T_0\left(\frac{x}{l}\right), \quad C = C_w = C_\infty + C_0\left(\frac{x}{l}\right), \tag{2.8}$$

$$M = M_w = M_\infty + M_0\left(\frac{x}{l}\right), \text{ at } y = 0, \quad T \to T_\infty, C \to C_\infty, M \to M_\infty, \text{ as } y \to \infty. \tag{2.9}$$

Here, u and v are the velocities in x and y directions, σ represents magnetic field strength, v and v_c indicate the viscosity of the fluid and microorganisms, D_m, D_B, D_n, and D_T are the chemical molecular diffusivity, Brownian, microorganisms, and thermal diffusions respectively, τ is the ratio between the heat capacity of the nanoparticle and the fluid, C_s is the concentration susceptibility, and C_p and ρ are the heat capacities and density of the fluid, κ' represents permeability constant, B_0 is the magnetic field strength, T and C are the fluid's temperature and concentration, M represents microorganisms mass density, g represents acceleration due to the gravity, $b > 0$ is a constant, $\beta > 0$ represents shrinking parameter, $\Gamma = (1/x)\ \Gamma_0$ indicates variable time and Γ_0 is a constant, l is the characteristic length, $\Phi = (l/x)(\partial u/\partial y)^2$ is the heat dissipation, κ indicates thermal conductivity, $\bar{\kappa}$ represents thermal diffusion ratio, β_T and β_C are the volumetric coefficients due to thermal and concentration expansions, and β_M indicates microorganisms coefficient. In addition, T_w, C_w, M_w are the wall temperature, concentration, density of microorganisms while T_∞, C_∞, M_∞ are the corresponding quantities outside the boundary layer respectively.

Let us introduce the following transformations:

$$u = b\left(\frac{x}{l}\right)f'(\eta), \quad v = -\sqrt{\frac{bv}{l}}f(\eta), \quad \eta = \sqrt{\frac{b}{vl}}y, \quad \theta(\eta) = \frac{T - T_\infty}{T_w - T_\infty}, \quad \varphi(\eta) = \frac{C - C_\infty}{C_w - C_\infty}, \quad \chi(\eta) = \frac{M - M_\infty}{M_w - M_\infty}. \tag{2.10}$$

Then the set of Eqs. (2.1)-(2.10) are converted into the following:

$$f''' + ff'' - (f')^2 + \sqrt{2}\ We f'' f''' - \left(Ha^2 + \bar{K}\right)f' + Gr_T\theta + Gr_C\varphi + Gr_M\chi = 0, \tag{2.11}$$

$$\left(1 + \frac{4}{3}R\right)\theta'' + Pr\, f\theta' - Pr\, f'\theta + EcPr\left(f''\right)^2 + PrN_b\theta'\varphi' + PrN_t\left(\theta'\right)^2 + PrD_f\varphi'' = 0, \tag{2.12}$$

$$\frac{1}{S_c}\varphi'' + f\varphi' - f'\varphi + \frac{1}{S_c}\frac{N_t}{N_b}\theta'' = 0, \tag{2.13}$$

$$\chi'' + S_b\chi' f - S_b f'\chi - Pe\left[\left(\sigma_1 + \chi\right)\varphi'' + \chi'\varphi'\right] = 0, \tag{2.14}$$

where

$$Gr_T = \frac{g\beta_T T_0 l}{b^2}, \quad Gr_C = \frac{g\beta_C C_0 l}{b^2}, \quad Gr_M = \frac{g\beta_M M_0 l}{b^2}, \quad Ha^2 = \frac{\sigma l B_0^2}{b\rho}, \quad We = \frac{1}{\sqrt{v}}\left(\frac{b}{l}\right)^{\frac{3}{2}}\Gamma_0, \quad \bar{K} = \frac{vl}{b\kappa'}, \quad Ec = \frac{b^2}{C_p T_0}, \quad N_b = \frac{\tau D_B}{C_s C_p v}\frac{(C_w - C_\infty)}{(T_w - T_\infty)}, \quad \alpha = \frac{\kappa}{\rho C_p}, \quad Pr = \frac{v}{\alpha'},$$

$$D_f = \frac{D_M \bar{\kappa}}{C_s C_p \nu}\frac{(C_w - C_\infty)}{(T_w - T_\infty)}, \quad q_r = -\frac{4\sigma^*}{3k^*}\frac{\partial T^4}{\partial y},$$
$$N_t = \frac{\tau D_T}{C_s C_p \nu}\frac{(M_w - M_\infty)}{\nu T_\infty}, \quad T^4 = 4T_\infty^4 T - 3T_\infty^4,$$
$$R = \frac{4\sigma^* T_\infty^3}{kk^*}, \quad v_w = -\sqrt{\frac{b\nu}{l}}S,$$
$$Sc = \frac{\nu}{D_B}, \quad Pe = \frac{bv_C}{D_n},$$
$$Sb = \frac{\nu}{D_n}, \quad \sigma_1 = \frac{M_\infty}{b(M_w - M_\infty)},$$

with boundary conditions:

$$f(0) = S, f'(0) = -\beta, \quad \theta(0) = 1, \varphi(0) = 1, \chi(0) = 1, \tag{2.15}$$

$$f'(\eta) \to 0, \theta(\eta) \to 0, \quad \varphi(\eta) \to 0, \chi(\eta) \to 0, \text{ as } \eta \to 0, \tag{2.16}$$

where S is the suction or injection parameter.

Here *Ha, Pr, Ec, D_f, We, Pe,* and *Sc* are the Hartman, Prandtl, Eckert, Dufour, Weissenberg, Peclet, and Schmidt numbers, $\bar{K}$ is the permeability constant, Gr_T, Gr_C and Gr_M are the constant dimensionless momentum, concentration, and microorganisms buoyancy parameters, respectively, N_b and N_t are the Brownian and thermophoretic diffusivity numbers, R is the radiation parameter, *Sb* is Schmidt number for microorganisms diffusivity and σ_1 is the mass concentration parameter. The physical meaning of these parameters is described in [18-26].

In addition, the dimensionless numbers such as local skin friction coefficient (Malik et al. [27]), local Nusselt number (Malik et al. [27]), local Sherwood number (Yusuf et al. [15]), and local density number of the microorganisms (Yusuf et al. [15]) are defined by

$$\left.\begin{aligned} Re_x^{1/2} C_f &= 2 * f''(0) + We\left(f''^{(0)}\right)^2 \\ Re_x^{-1/2} Nu_x &= -\theta'(0) \\ Re_x^{-1/2} Sh_x &= -\varphi'(0) \\ Re_x^{-1/2} Nn_x &= -\chi'(0) \end{aligned}\right\} \tag{2.17}$$

where, Re_x is the local Reynolds number.

Here, the local skin friction coefficient quantifies the amount of frictional force per unit area that is generated by the fluid flow along a solid boundary; the local Nusselt number quantifies the effectiveness of convective heat transfer relative to conductive heat transfer in a fluid near a solid surface; the local Sherwood number is the ratio of the convective mass transfer to the rate of diffusive mass transport.

3. Numerical Techniques

In this research, resulting non-dimensional nonlinear ODEs (Eqs. (2.11)-(2.14)) along with the boundary conditions (Eqs. (2.15)-(2.16)) are transformed into a first-order system of ODEs and then solved using the nonlinear shooting method with RK 4th order scheme (Burden & Faires [28]). To convert the Eqs. (2.11) - (2.14) into first-order ODEs, let us introduce the following transformations:

$$f = u_1, f' = u_2, f'' = u_3, \quad \theta = u_4, \theta' = u_5, \varphi = u_6, \quad \varphi' = u_7, \chi = u_8, \chi' = u_9. \tag{3.1}$$

Using the above transformations, we get the following system of ODEs:

$$\left.\begin{aligned} u_1' &= u_2, \\ u_2' &= u_3, \\ u_3' &= \frac{\left(Ha^2 + \bar{K}\right)u_2 + u_2^2 - u_1 u_3 - Gr_T u_4 - Gr_C u_6 - Gr_M u_8}{1 + \sqrt{2} We u_3}, \\ u_4' &= y_5, \\ u_5' &= \frac{-Pr\left(u_1 u_5 + Ecu_3^2 + D_f u_7' + N_b u_5 u_7 + N_t u_5^2\right)}{1 + \frac{4}{3}R}, \\ u_6' &= u_7, \\ u_7' &= -Sc\left(u_1 u_7 + \frac{1}{Sc}\frac{N_t}{N_b}u_5'\right), \\ u_8' &= u_9, \\ u_9' &= Pe\left\{\left(\sigma_1 + u_8\right)u_7' + u_7 u_9\right\} - Sbu_1 u_9, \end{aligned}\right\}$$

and the corresponding boundary conditions are

$$\begin{aligned}&\text{At } \eta = 0:\\ &u_1 = S, u_2 = -\beta,\\ &u_4 = 1, u_6 = 1, u_8 = 1.\\ &\text{As } \eta \to \infty:\\ &u_2 \to 0, u_4 \to 0, u_6 \to 0, u_8 \to 0.\end{aligned} \tag{3.2}$$

4. Validation

The proposed numerical method is validated against the results of Grubka and Bobba [29], Ishak et al. [30], and El-Aziz [31], and the results are presented in Table 1. A very strong agreement is observed from the results in Table 1.

Table 1. Results of $-\theta'(0)$ with the variation of *Pr*.

Pr	Grubka and Bobba [29]	Ishak et al. [30]	El-Aziz [31]	Present method
0.72	0.8086	0.8086	0.80873	0.808637
1.0	1.0000	1.0000	1.00000	0.999999
3.0	1.9237	1.9237	1.92368	1.923677
10.0	3.7207	3.7207	3.72067	3.720661
100.0	12.294	12.2941	12.29408	12.294167

5. Results and Discussion

Here the parameters are considered as

$$Pr = 0.7, N_t = 0.1, Pe = 1.0, Gr_T = 1.0,$$
$$Gr_C = Gr_M = 0.5, Sc = Sb = 1.0,$$

while the others are mentioned in the captions of the following figures. Also, other values of *Pr* such as *Pr* = 7.0, 21.0 are considered for this study [32, 33].

Table 2. Variation of $Re_x^{1/2}C_f, Re_x^{-1/2}Nu_x, Re_x^{-1/2}Sh_x$ and $Re_x^{-1/2}Nn_x$ for β = 5.0, N_t = 0.1, *Pe* = 1.0, Gr_T = 1.0, Gr_C = Gr_M =0.5, *Sc* = *Sb* =1.0.

Pr	*S*	*Ha*	N_b	D_f	*Ec*	*We*	*R*	$f''(0)$	$-\theta'(0)$	$-\varphi'(0)$	$-\chi'(0)$
0.7	7.0	0.4	0.5	0.1	0.1	0.05	0.5	18.21468	−0.44928	6.04945	12.33632
							1.0	18.30340	−0.32919	6.03967	12.33004
							2.0	18.46831	−0.21484	6.03626	12.33196
0.7	7.0	0.4	0.5	0.1	0.1	0.00	1.0	32.17404	−1.04239	6.40915	12.82613
						0.05		18.30209	−0.32811	6.03969	12.33005
						0.10		14.30351	−0.12789	5.87421	12.10093
0.7	7.0	0.3	0.5	0.1	0.0	0.05	1.0	18.19924	1.23838	5.70018	11.98199
					0.1			18.26551	−0.32701	6.03816	12.32797
					0.3			18.39708	−3.49494	6.72176	13.02724
0.7	7.0	0.5	0.5	0.0	0.3	0.05	1.0	18.40696	−1.72122	6.34106	12.63894
				0.5				18.45319	−2.72039	6.55709	12.86024
				1.0				18.49902	−3.78555	6.78650	13.09501
0.7	7.0	0.5	0.2	0.5	0.2	0.05	1.0	18.39783	−1.10816	6.51215	12.80615
			0.4					18.38863	−1.08769	6.25523	12.55027
			0.6					18.38726	−1.09319	6.17383	12.46922
0.7	7.0	0.0	0.5	0.1	0.1	0.05	1.0	18.21507	−0.32309	6.03621	12.32530
		0.5						18.35056	−0.33091	6.04163	12.33269
		1.0						18.74224	−0.35381	6.05718	12.35392
0.7	6.0	0.4	0.5	0.1	0.1	0.05	1.0	15.69574	−0.45222	4.84781	9.98765
	8.0							20.62536	−0.21816	7.16076	14.54904
	10.0							24.73340	−0.00567	9.30088	18.80949
0.7	7.0	0.4	0.5	0.1	0.1	0.05	1.0	18.21008	−0.45768	6.05030	12.33697
7.0								18.01496	−2.99221	6.48886	12.75621
21.0								17.99366	−9.69470	7.81268	14.06442

Effects of Weissenberg number on the coefficients of $Re_x^{1/2}C_f$, $Re_x^{-1/2}Nu_x$, $Re_x^{-1/2}Sh_x$ and $Re_x^{-1/2}Nn_x$ are shown in Fig. 2 and Table 2. It is evident that for increasing We the heat transfer increases and the remaining quantities decrease. On the other hand, increasing in β augments the skin friction coefficient and reduces the heat transfer. In addition, values of

$Re_x^{-1/2}Sh_x$ and $Re_x^{-1/2}Nn_x$ are found to decrease except that these have a decreasing and increasing tendency for $We < 0.03$. Results also expose that dual solutions occur in a narrower domain for higher values of We, which indicates that boundary layer separation is accelerated with the increase of *We*. This is due to the fact that the value of *We* is higher either for lower kinematic viscosity or for higher shrinking velocity. Such findings could be correlated with aforesaid viscous fluid or engineering applications like cooling or drying of papers, hot rolling, wire drawing, cooling of an infinite metallic plate in a cooling bath, in textile and glass fiber production and in metallurgy. It is mentioned here that the solid lines represent the stable solutions and dashed lines represent unstable solutions. However, unstable solutions cannot be interpreted from a practical point of view and so these are not acceptable solutions.

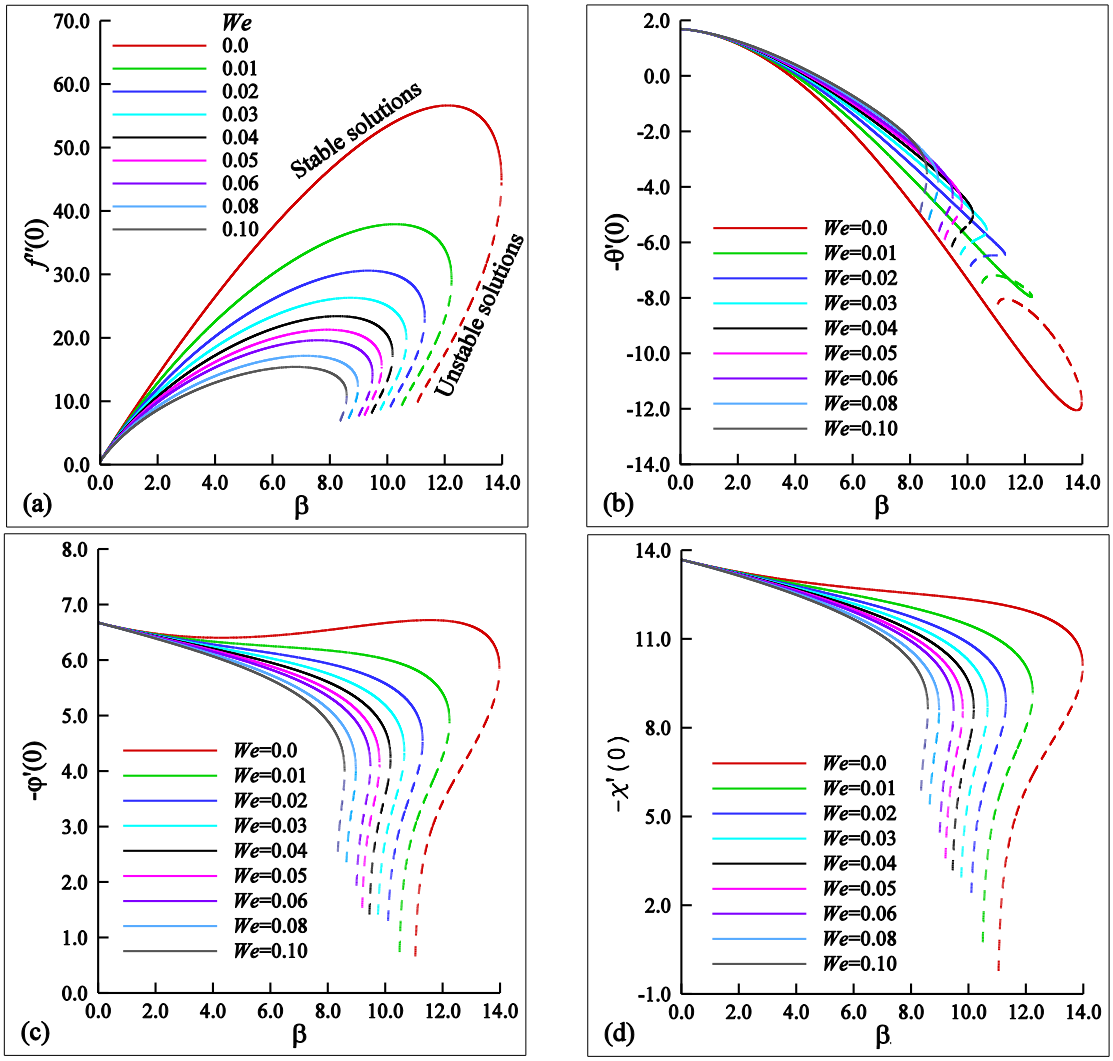

Fig. 2. Effects of *We* on the coefficients of $Re_x^{1/2}C_f$, $Re_x^{-1/2}Nu_x$, $Re_x^{-1/2}Sh_x$ and $Re_x^{-1/2}Nn_x$ for $S = 7.0$, $Ec = 0.1$, $N_b = 0.5$, $Ha = 0.4$, $D_f = 0.1$, $R = 1.0$.

In Fig. 3 and Table 2, variations of the coefficients of $Re_x^{1/2}C_f$, $Re_x^{-1/2}Nu_x$, $Re_x^{-1/2}Sh_x$ and $Re_x^{-1/2}Nn_x$ with the change of the suction parameter are presented. For higher values of S, the coefficients of $Re_x^{1/2}C_f$, $Re_x^{-1/2}Nu_x$, $Re_x^{-1/2}Sh_x$ and $Re_x^{-1/2}Nn_x$ are found to increase. Dual solutions exist in a broader domain of β owing to the increase of S. The cause for the aforesaid characteristics is that the higher mass flux through the permeable sheet diminishes the boundary layer separation. It indicates that the volumetric mass flux through a sheet can be considered to be a tuning parameter for running a system.

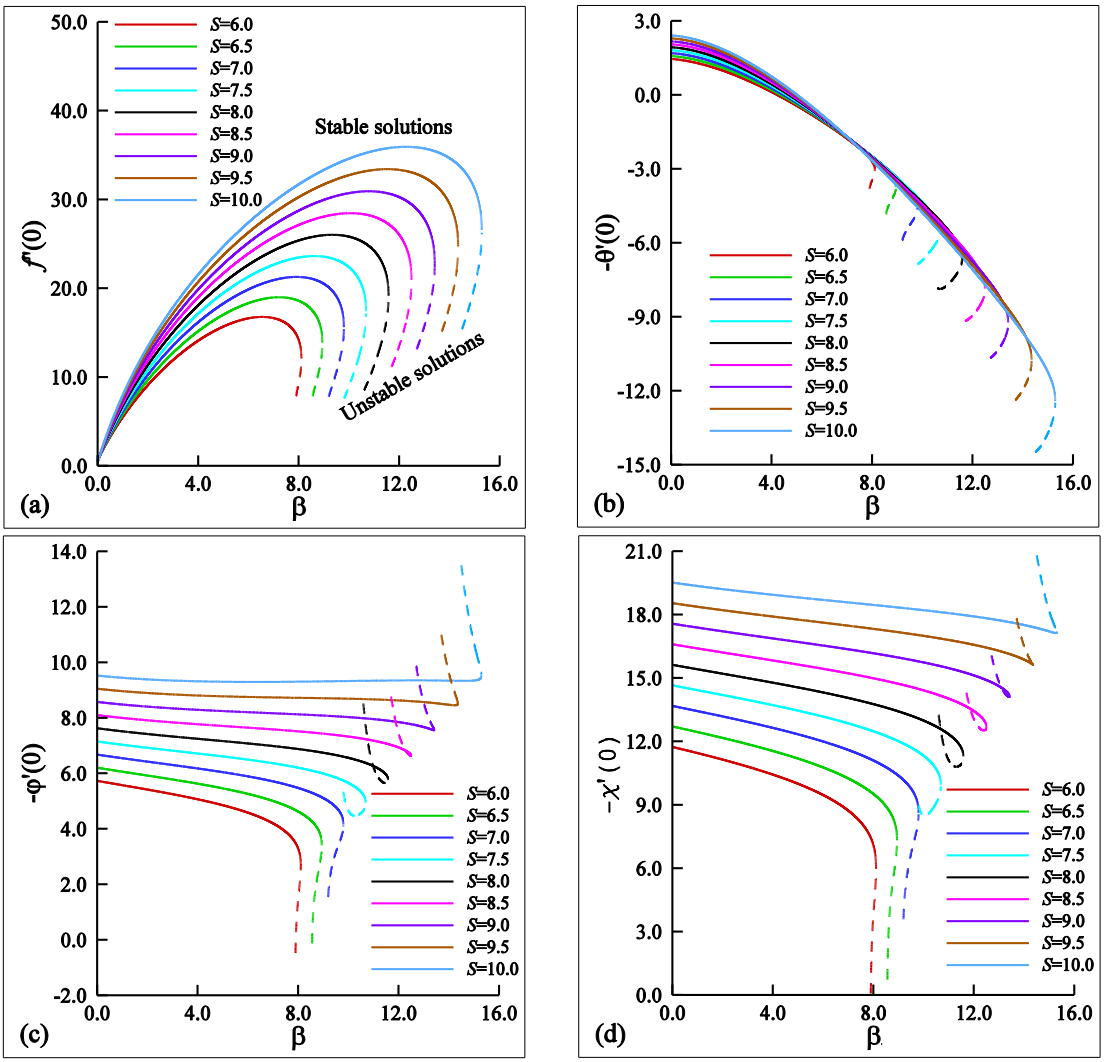

Fig. 3. Effects of S on the coefficients of $Re_x^{1/2}C_f$, $Re_x^{-1/2}Nu_x$, $Re_x^{-1/2}Sh_x$ and $Re_x^{-1/2}Nn_x$ for We = 0.05, Ec = 0.1, N_b = 0.5, Ha = 0.4, D_f = 0.1, R = 1.0.

The influences of the radiation parameter, R, on the coefficients of $Re_x^{1/2}C_f$, $Re_x^{-1/2}Nu_x$, $Re_x^{-1/2}Sh_x$ and $Re_x^{-1/2}Nn_x$ are elucidated in Fig. 4 and Table 2. Results show that the value of the coefficient of $Re_x^{1/2}C_f$, is always higher over the domain of β due to the increase of R. But the larger value of R leads to a decrease in $Re_x^{-1/2}Nu_x$ over a certain domain of β and after that it increases with R. The converse scenario is observed in the changes

of $Re_x^{-1/2}Sh_x$ and $Re_x^{-1/2}Nn_x$ with respect to R. In addition, the existence of dual solutions is elongated in the domain of β for higher values of R.

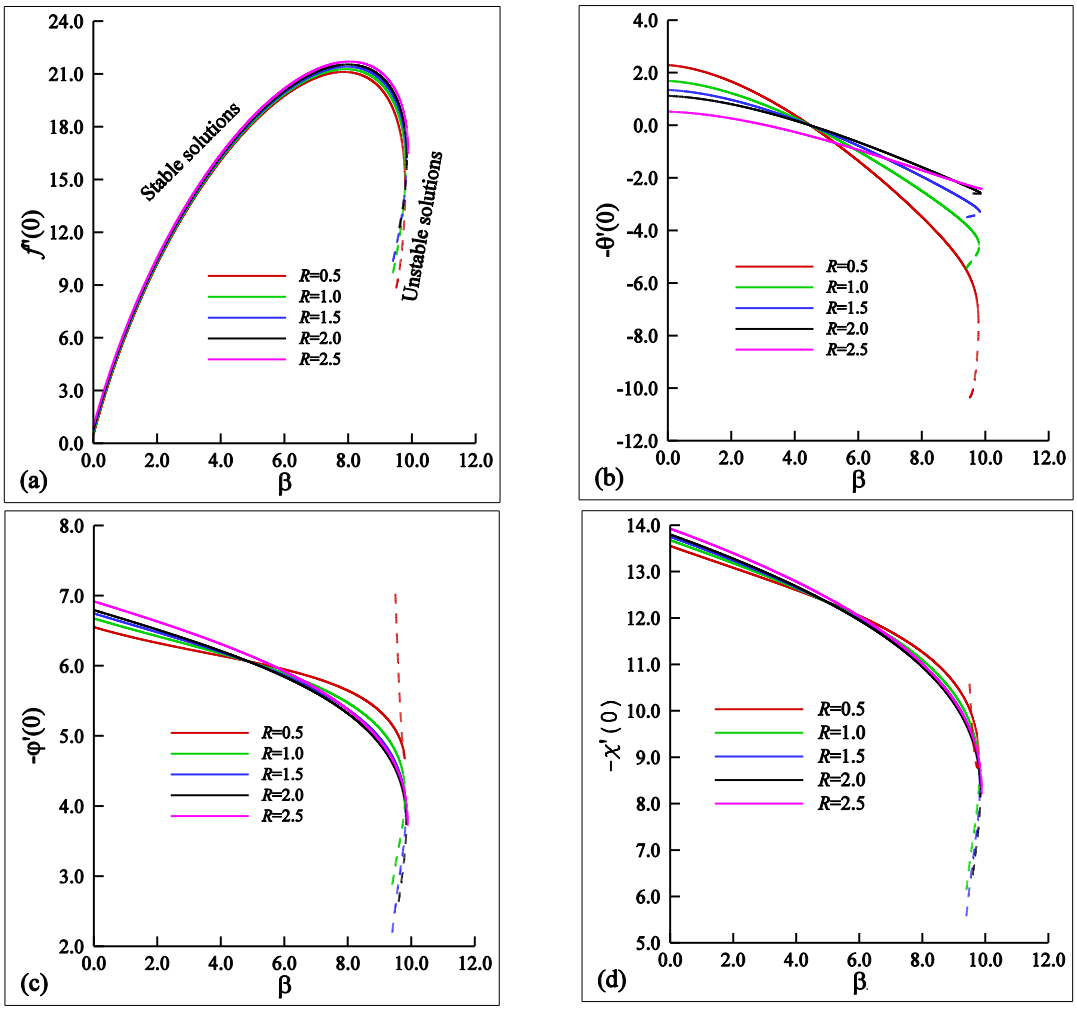

Fig. 4. Effects of R on the coefficients of $Re_x^{1/2}C_f$, $Re_x^{-1/2}Nu_x$, $Re_x^{-1/2}Sh_x$ and $Re_x^{-1/2}Nn_x$ for We = 0.05, S = 5.0, Ec = 0.1, N_b = 0.5, Ha = 0.4, D_f = 0.1.

Fig. 5 and Table 2 illustrate the impacts of Ec on the coefficients of $Re_x^{1/2}C_f$, $Re_x^{-1/2}Nu_x$, $Re_x^{-1/2}Sh_x$ and $Re_x^{-1/2}Nn_x$. An increase in Ec causes a decrease in heat transfer but significantly augments the value of the coefficients of $Re_x^{1/2}C_f$, $Re_x^{-1/2}Sh_x$ and $Re_x^{-1/2}Nn_x$. For lower values of Ec, values of $Re_x^{-1/2}Sh_x$ and $Re_x^{-1/2}Nn_x$ monotonically decreases against β, whereas they exhibit decreasing and increasing patterns on β for higher values of Ec. By definition, Ec is the ratio of advective transport to heat dissipation potential. Consequently, higher Ec corresponds to stonger advection of kinetic energy or lower heat dissipation. That is why, heat transfer decreases with increasing Ec. It is also noted that differences of the values of the coefficients of $Re_x^{1/2}C_f$, $Re_x^{-1/2}Nu_x$, $Re_x^{-1/2}Sh_x$ and $Re_x^{-1/2}Nn_x$ corresponding to two distinct Ec values increase considerably for higher values of β.

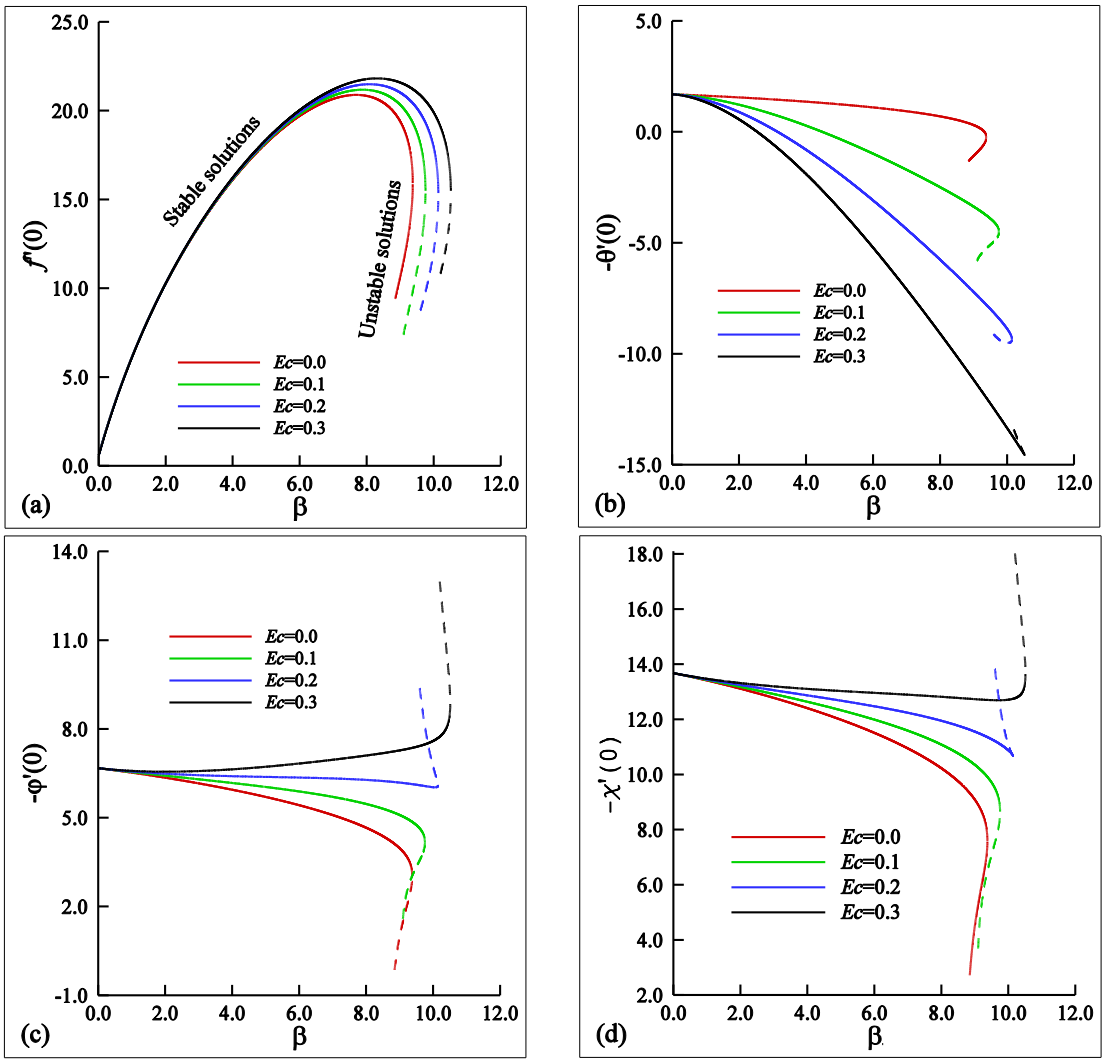

Fig. 5. Effects of Ec on the coefficients of $Re_x^{1/2}C_f$, $Re_x^{-1/2}Nu_x$, $Re_x^{-1/2}Sh_x$ and $Re_x^{-1/2}Nn_x$ for We = 0.05, S = 7.0, N_b = 0.5, Ha = 0.3, D_f = 0.1, R = 1.0.

Effects of D_f on the coefficients of $Re_x^{1/2}C_f$, $Re_x^{-1/2}Nu_x$, $Re_x^{-1/2}Sh_x$ and $Re_x^{-1/2}Nn_x$ are demonstrated in Fig. 6 and Table 2. It is seen that when D_f is increased, the values of the coefficients of $Re_x^{1/2}C_f$, $Re_x^{-1/2}Sh_x$ and $Re_x^{-1/2}Nn_x$ are increased and the values of $Re_x^{-1/2}Nu_x$ are decreased. The domain of the existence of dual solutions is increased a little bit for increasing values of D_f. The reason for such characteristics is that a larger D_f implies higher chemical mass diffusion and consequently the values of $Re_x^{-1/2}Sh_x$ and $Re_x^{-1/2}Nn_x$ are increased with increasing D_f.

Fig. 7 and Table 2 depict the changes of the coefficients of $Re_x^{1/2}C_f$, $Re_x^{-1/2}Nu_x$, $Re_x^{-1/2}Sh_x$ and $Re_x^{-1/2}Nn_x$ for different values of Ha. Increasing in Ha gives rise to an increase in the coefficients of $Re_x^{1/2}C_f$, $Re_x^{-1/2}Sh_x$ and $Re_x^{-1/2}Nn_x$, but a decrease in $Re_x^{-1/2}Nu_x$. The domain of dual solutions is broadened by the increase of Ha. This is because stronger magnetic field accelerates the fluid flow and thereby the fluid gets attached to the sheet and the flow separation delays.

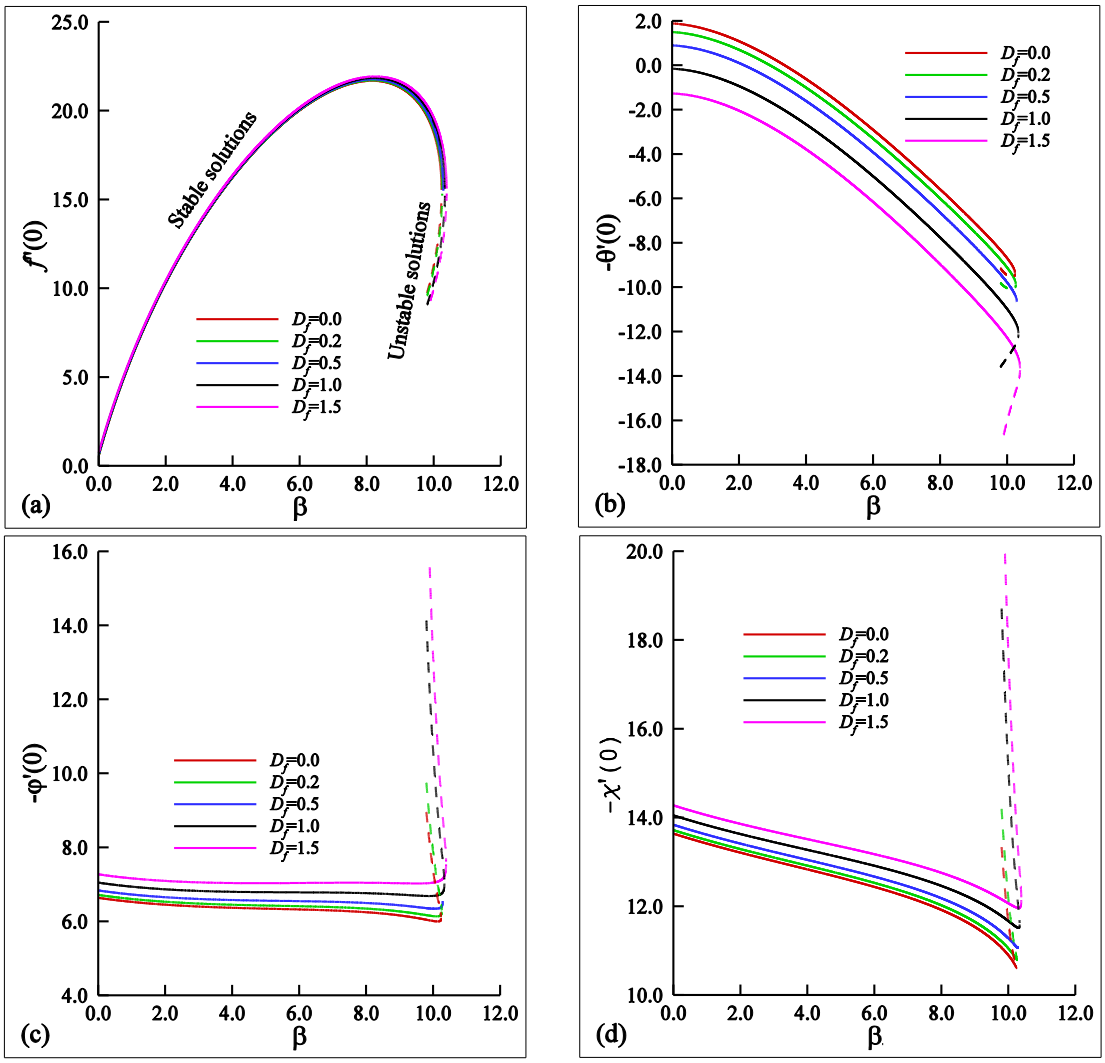

Fig. 6. Effects of D_f on the coefficients of $Re_x^{1/2}C_f$, $Re_x^{-1/2}Nu_x$, $Re_x^{-1/2}Sh_x$ and $Re_x^{-1/2}Nn_x$ for We = 0.05, S = 7.0, Ec = 0.2, N_b = 0.5, Ha = 0.5, R = 1.0.

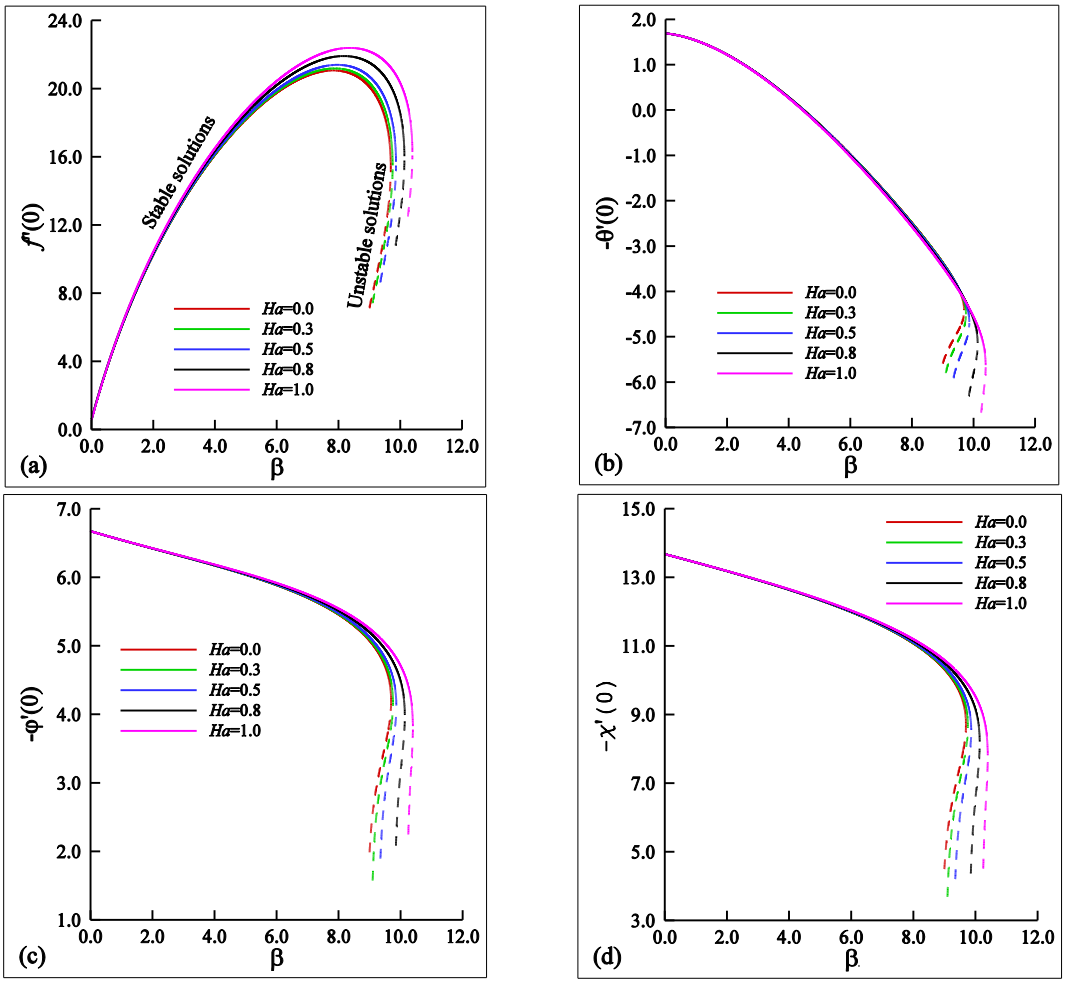

Fig. 7. Effects of *Ha* on the coefficients of $Re_x^{1/2}C_f$, $Re_x^{-1/2}Nu_x$, $Re_x^{-1/2}Sh_x$ and $Re_x^{-1/2}Nn_x$ for $We = 0.05$, $S = 7.0$, $Ec = 0.1$, $N_b = 0.5$, $D_f = 0.1$, $R = 1.0$.

The effects of the Brownian diffusivity number, Nb, on the coefficients of $Re_x^{1/2}C_f$, $Re_x^{-1/2}Nu_x$, $Re_x^{-1/2}Sh_x$ and $Re_x^{-1/2}Nn_x$ are elucidated in Fig. 8. It is evident from these figures and Table 2 that there is weak influence of Nb on the local skin friction coefficient. For increasing Nb, values of $Re_x^{-1/2}Sh_x$ and $Re_x^{-1/2}Nn_x$ are found to be higher in a small domain, and then they substantially decrease. The converse behavior is observed for $Re_x^{-1/2}Nu_x$ with the change of Nb. However, a very little increase in the domain of dual solutions is observed for higher values of Nb.

The variations in the coefficients of $Re_x^{1/2}C_f$, $Re_x^{-1/2}Nu_x$, $Re_x^{-1/2}Sh_x$, and $Re_x^{-1/2}Nn_x$ with the change of the Prandtl number, *Pr*, are depicted in Fig. 9 and Table 2. Results show that the Prandtl number strongly affects all the quantities. An increase in *Pr*, values of the coefficients of $Re_x^{1/2}C_f$, $Re_x^{-1/2}Sh_{,x}$ and $Re_x^{-1/2}Nn_x$ decrease. However, the value of $Re_x^{-1/2}Nu_x$ significantly decreases for higher Pr. The quantities $Re_x^{-1/2}Nu_x$, $Re_x^{-1/2}Sh_x$ and $Re_x^{-1/2}Nn_x$ show distinct behavior for larger *Pr* relative to smaller *Pr*. Specifically, when *Pr* (=0.7) is small, values of $Re_x^{-1/2}Sh_x$ and $Re_x^{-1/2}Nn_x$ always decrease with the increase of β, whereas for higher *Pr* (=7.0 and 21.0) they first increase and then decrease along β.

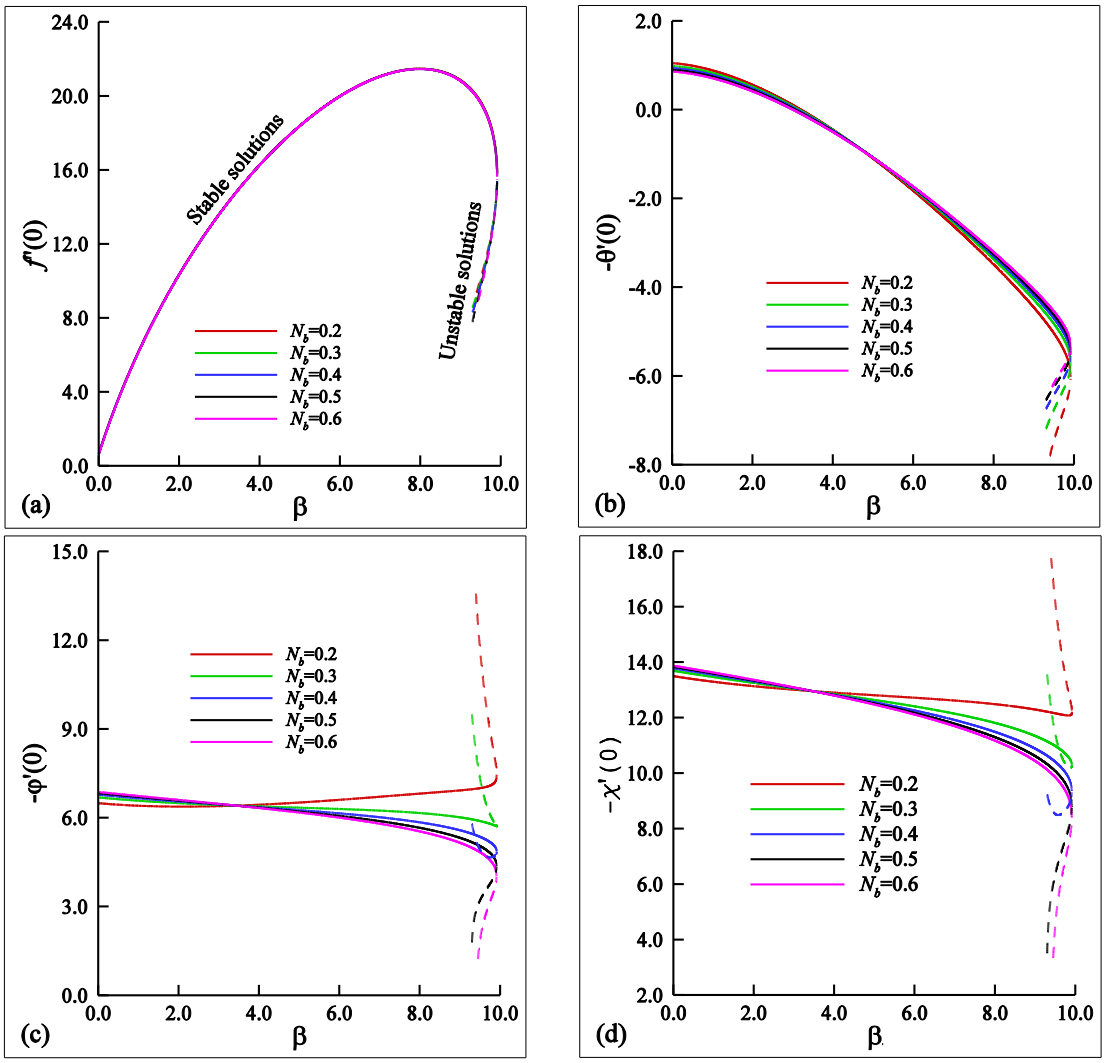

Fig. 8. Effects of N_b on the coefficients of $Re_x^{1/2}C_f$, $Re_x^{-1/2}Nu_x$, $Re_x^{-1/2}Sh_x$ and $Re_x^{-1/2}Nn_x$ for $We = 0.05$, $Ha = 0.5$, $S = 7.0$, $Ec = 0.2$, $N_t = 0.1$, $D_f = 0.5$, $R = 1.0$.

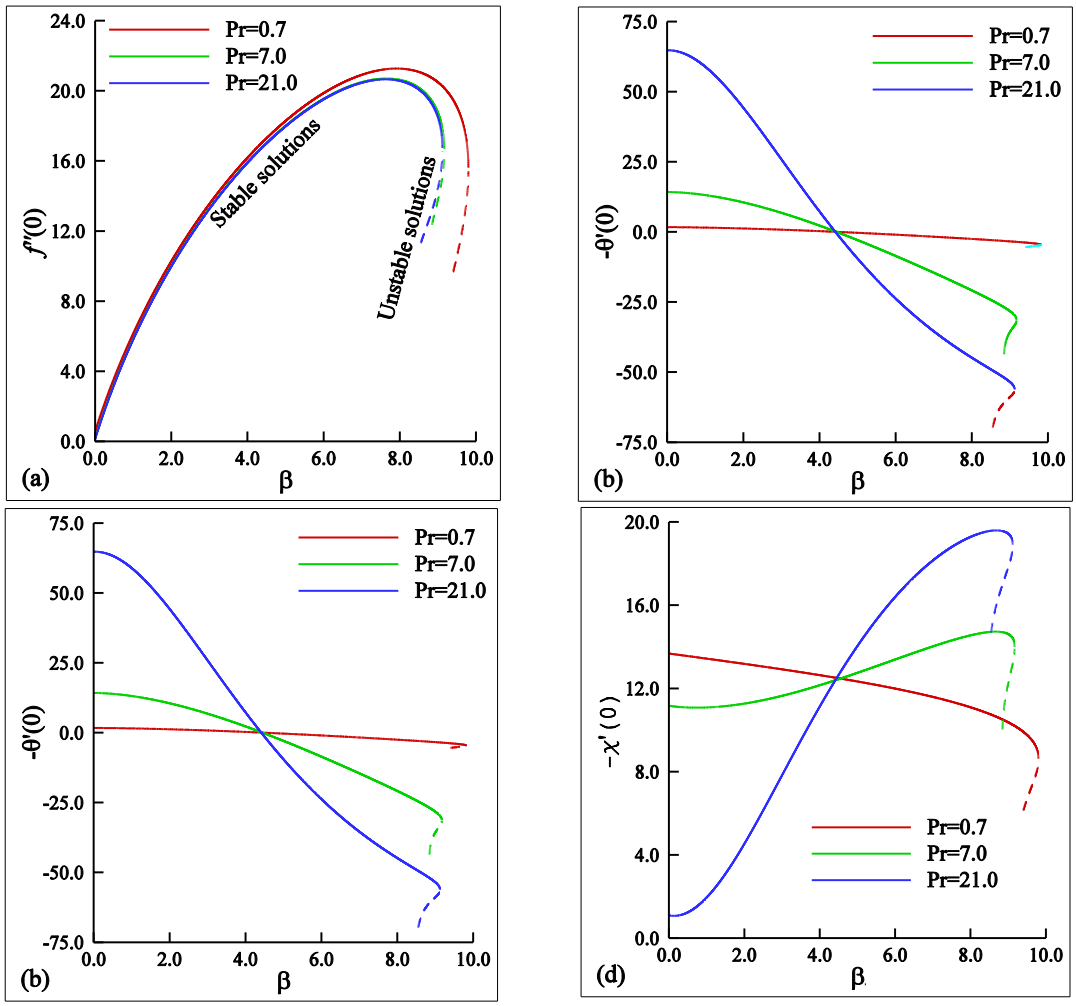

Fig. 9. Effects of N_b on the coefficients of $Re_x^{1/2}C_f$, $Re_x^{-1/2}Nu_x$, $Re_x^{-1/2}Sh_x$ and $Re_x^{-1/2}Nn_x$ for $We = 0.05$, $Ha = 0.4$, $S = 7.0$, $Ec = 0.1$, $N_t = 0.1$, $N_b = 0.5$, $D_f = 0.1$, $R = 1.0$.

6. Conclusion

In this investigation, dual solutions of a Williamson fluid flow mixed with microorganisms over a permeable shrinking sheet are examined in the presence of the magnetic field, radiation, Dufour effect, heat dissipation, and Brownian diffusion. Similarity transformations are introduced to reduce the governing equations into a set of differential equations which are solved using the shooting technique along with the Runge-Kutta method. The following findings are observed:

- $Re_x^{1/2}C_f$, $Re_x^{-1/2}Sh_x$, and $Re_x^{-1/2}Nn_x$ are considerably increased owing to the increase of Ec, D_f, and Ha. In this case, $Re_x^{-1/2}Nu_x$ is found to diminish. The converse is recognized for increasing We.
- Increasing S substantially augments $Re_x^{1/2}C_f$, $Re_x^{-1/2}Nu_x$, $Re_x^{-1/2}Sh_x$, and $Re_x^{-1/2}Nn_x$.
- Domain of the existence of dual solutions broadens with higher S, Ec and Ha. But it shrinks with larger We.
- Results indicate that We, S, Ec, and Ha are the important parameters for the considered problem.

Nomenclature:

B_0	Magnetic field strength
C	Fluid's concentration
C_s	Concentration susceptibility
C_p	Heat capacities of the fluid
D_m, D_B, D_n,, D_T	Chemical molecular diffusivity, Brownian, microorganisms, and thermal diffusions
D_f	Dufour number
Ec	Eckert number
g	Acceleration due to the gravity
Gr_T, Gr_C, Gr_M	Momentum, concentration, and microorganisms buoyancy parameters
Ha	Hartman number
$\bar{\kappa}$	Thermal diffusion ratio
$\bar{\mathrm{K}}$	Permeability constant
M	Microorganisms mass density
N_b & N_t	Brownian and thermophoretic diffusivity numbers
Nn	Density number of the microorganisms
Nu	Nusselt number
Pe	Peclet number
Pr	Prandtl number
R	Radiation parameter
Re	Reynolds number
S	Suction or injection parameter
Sb	Schmidt number for microorganisms diffusivity
Sc	Schmidt number
Sh	Sherwood number
T	Fluid's temperature
T_w, C_w, M_w	Wall temperature, concentration, density of microorganisms
T_∞, C_∞, M_∞	Temperature, concentration, density of microorganisms outside the boundary layer
u & v	Velocities in x and y directions
We	Weissenberg number
σ	Magnetic field strength
ν & ν_c	Viscosity of the fluid and microorganisms
τ	Ratio between the heat capacity of the nanoparticle and the fluid
ρ	Density of the fluid
κ'	Permeability constant
b, Γ_0	Constant
β	Shrinking parameter
Γ	Variable time
l	Characteristic length
Φ	Heat dissipation
κ	Thermal conductivity
β_T & β_C	Volumetric coefficients due to thermal and concentration expansions
β_M	Microorganisms coefficient
σ_1	Mass concentration parameter

References

[1] Nadeem S, Hussain ST. Flow and heat transfer analysis of Williamson nanofluid. Applied Nanoscience 2014;4;1005-12.

[2] Krishnamurthy MR, Prasannakumara BC, Gireesha BJ, Gorla RSR. Effect of chemical reaction on MHD boundary layer flow and melting heat transfer of Williamson nanofluid in porous medium. Engineering Science and Technology, an International Journal 2016;19(1);53-61.

[3] Ibrahim W, Gamachu D. Nonlinear convection flow of Williamson nanofluid past a radially stretching surface. AIP Advances 2019;9;1-13.

[4] Reddy CS, Naikoti K, Rashidi MM. MHD flow and heat transfer characteristics of Williamson nanofluid over a stretching sheet with variable thickness and variable thermal conductivity. Transactions of A. Razmadze Mathematical Institute 2017;171(2);195-211.

[5] Shawky HM, Eldabe NTM, Kamel KA, Abd-Aziz EA. MHD flow with heat and mass transfer of Williamson nanofluid over stretching sheet through porous medium. Microsystem Technologies 2019;25; 1155-69.

[6] Kho YB, Hussanan A, Mohamed MKA, Salleh MZ. Heat and mass transfer analysis on flow of Williamson nanofluid with thermal and velocity slips: Buongiorno model. Propulsion and Power Research 2019;8(3);243-52.

[7] Zaib A, Abelman S, Chamkha AJ, Rashidi MM. Entropy generation of Williamson nanofluid near a stagnation point over a moving plate with binary chemical reaction and activation energy. Heat Transfer Research 2018;49(11);1131-49.

[8] Zaib A, Haq RU, Chamkha AJ, Rashidi MM. Impact of nonlinear radiative nanoparticles on an unsteady flow of a Williamson fluid toward a permeable convectively heated shrinking sheet. World Journal of Engineering 2018;15(6);731-42.

[9] Dawar A, Shah Z, Islam S. Mathematical modeling and study of MHD flow of Williamson nanofluid over a nonlinear stretching plate with activation energy. Heat Transfer 2021;50;2558-70.

[10] Mishra SR, Mathur P, Williamson nanofluid flow through porous medium in the presence of melting heat transfer boundary condition: Semi-analytical approach. Multidiscipline Modeling in Materials and Structures 2021; 17(1);19-33.

[11] Ahmed K, Akbar T. Numerical investigation of magneto-hydrodynamics Williamson nanofluid flow over an exponentially stretching surface. Advances in Mechanical Engineering 2021;13(5);1-12.

[12] Qureshi MA. Numerical simulation of heat transfer flow subject to MHD of Williamson nanofluid with thermal radiation. Symmetry 2021;13;10.

[13] Mehryan SAM, Kashkooli FM, Soltani M, Raahemifar K. Fluid flow and heat transfer analysis of a nanofluid containing motile gyrotactic micro-organisms passing a nonlinear stretching vertical sheet in the presence of a non-uniform magnetic field; Numerical approach. PLoS ONE 2016;11(6);e0157598.

[14] Biswas N, Datta A, Manna NK, Mandal D, Gorla R. Thermo-bioconvection of oxytactic microorganisms in porous media in the presence of magnetic field. International Journal of Numerical Methods for Heat & Fluid Flow 2021;31(5);1638-61.

[15] Yusuf TA, Mabood F, Prasannakumara BC, Sarris IE. Magneto-bioconvection flow of Williamson nanofluid over an inclined plate with gyrotactic microorganisms and entropy generation. Fluids 2021;6(3); 109.

[16] Yahaya RI, Arifin NM, Isa SSPM, Rashidi MM. Magnetohydrodynamics boundary layer flow of micropolar fluid over an exponentially shrinking sheet with thermal radiation: Triple solutions and stability

analysis. Mathematical Methods in the Applied Sciences 2021;44;10578-608.

[17] Parvin S, Isa SSPM, Arifin NM, Ali FM. The inclined factors of magnetic field and shrinking sheet in Casson fluid flow, Heat and Mass Transfer. Symmetry 2021;13(3); 373.

[18] Schlichting H, Gersten K. Boundary-layer theory, Springer Publication, 8th Edition, 2000.

[19] Cebeci T, Cousteix J. Modeling and computation of boundary-layer flows. Second Edition. Horizon Publishing, Springer, 2005.

[20] Telyakovskiy A. Approximate solutions to the Boussinesq equation: Similarity transformation approach. LAP LAMBERT Academic Publishing, 2011.

[21] Lienhard IV JH, Lienhard VJ, Heat transfer textbook, Cambridge Massachusetts Phlogiston Press, 4th Edition, 2017.

[22] Lund LA, Omar Z, & I. Khan. Analysis of dual solution for MHD flow of Williamson fluid with slippage. Heliyon 2019;5;e01345.

[23] Shah SAA, Awan AU. Significance of magnetized Darcy-Forchheimer stratified rotating Williamson hybrid nanofluid flow: A case of 3D sheet. International Communications in Heat and Mass Transfer 2022;136;106214.

[24] Yahya AU, Salamat N, Huang W-H, Siddique I, Abdal S, Hussain S. Thermal characteristics for the flow of Williamson hybrid nanofluid (MoS_2 + ZnO) based with engine oil over a stretched sheet. Case Studies in Thermal Engineering 2021;26; 101196.

[25] Hamid A, Hashim, Khan M, Hafeez A. Unsteady stagnation-point flow of Williamson fluid generated by stretching/shrinking sheet with Ohmic heating. International Journal of Heat and Mass Transfer 2018;126;933-40.

[26] Almaneea A. Numerical study on heat and mass transport enhancement in MHD Williamson fluid via hybrid nanoparticles. Alexandria Engineering Journal 2022;61(10);8343-54.

[27] Malik MY, Bibi M, Khan F, Salahuddin T. Numerical solution of Williamson fluid flow past a stretching cylinder and heat transfer with variable thermal conductivity and heat generation/absorption. AIP Advances 2016;6;035101.

[28] Burden RL, Faires JD. Numerical analysis. Ninth edition. ISBN-13: 978-0538-73351-9, CENGAGE Learning, 2010.

[29] Grubka LJ, Bobba KM. Heat transfer characteristics of a continuous stretching surface with variable temperature. ASME J. Heat Transfer 1985;107;248-50.

[30] Ishak A, Nazar R, Pop I. Boundary layer flow and heat transfer over an unsteady stretching vertical surface. Meccanica 2009;44; 369-75.

[31] El-Aziz MA. Mixed convection flow of a micropolar fluid from an unsteady stretching surface with viscous dissipation. J. Egypt. Math. Soc. 2013;21;385-94.

[32] Hashim, Khan M, Hamid A. Numerical investigation on time-dependent flow of Williamson nanofluid along with heat and mass transfer characteristics past a wedge geometry. International Journal of Heat and Mass Transfer 2018;118;480-91.

[33] Ganesh NV, Al-Mdallal QM, Kameswaran PK. Numerical study of MHD effective Prandtl number boundary layer flow of γ Al_2O_3 nanofluids past a melting surface. Case Studies in Thermal Engineering 2019; 13;100413.